Note

Crystal structures of amarine and isoamarine and copper(I) coordination chemistry with their allylation products

Xue-Feng Huang [1], Yu-Mei Song [1], Xi-Sen Wang [1], Jie Pang, Jing-Lin Zuo, Ren-Gen Xiong [*]

Coordination Chemistry Institute, The State Key Laboratory of Coordination Chemistry, Nanjing University, Hankou Road, Nanjing, Jiangsu 210093, PR China

Abstract

The crystal structures of amarine (**1**) and isoamarine (**2**), important intermediates in the preparation of 1,2-diphenyl-diaminoethane, were successfully determined. Their allylation products, 1,3-diallyl amarine (**1**)(CH$_2$─CH═CH$_2$)$_2$Br (**3**) and isoamarine bromide (**2**)(CH$_2$─CH═CH$_2$)$_2$Br (**4**) [the crystal structures of (**1**)(CH$_2$─CH═CH$_2$)$_2$PF$_6$(**3-Br + PF$_6$**) and (**2**)(CH$_2$─CH═CH$_2$)$_2$PF$_6$ (**4-Br + PF$_6$**) are also successfully determined to confirm allylation products], react with CuBr to afford (**1**)$_2$(CH$_2$─CH═CH$_2$)$_4$(Cu$_2$Br$_4$) (**5**) and (**2**)(CH$_2$─CH═CH$_2$)$_2$(Cu$_2$Br$_3$) (**6**), respectively. Crystal structures of **5** and **6** reveal that **5** is an anion discrete complex without olefin moiety coordination, and **6** has a 1D infinite chain with olefin moiety coordination as a bridging spacer. The fluorescent emission spectra of **5** ($\lambda_{emax} = 570$ nm) and **6** ($\lambda_{emax} = 642$ nm) were measured, and display a significant difference that can be used for solid state fluorescent sensing them.
© 2005 Elsevier B.V. All rights reserved.

Keywords: Amarine; Isoamarine; Allylation; Copper(I) olefin complex; Crystal structures; Fluorescent emission

1. Introduction

Chiral 1,2-diphenyl-diaminoethane (stilbenediamine, stein) have been widely used in enantioselective catalysis as a very useful chelating ligands [1], such as the enantioselective titanium-mediated addition of diethylzinc to aldehydes [2a], the V complexes with tetradentate Schiff base ligands containing optically active stein [2b], and optically active β-ketoiminato cobalt complexes with optically active stein as effective Lewis acid catalysts for enantioselective hetero Diels–Alder reactions [2c]. On the other hand, the olefin-copper(I) complex with chiral bidentate ligand (1S,2S)-*N,N'*-bis-(mesitylmethyl)-1,2-diphenyl-1,2-ethanediamine has been used to resolve racemic 1-buten-3-ol [3]. Consequently, the preparation of racemic stein demonstrates the great importance. Corey and coworkers [4]

reported a simplified synthesis of racemic stein from benzaldehyde and liquid ammonia, and determined the crystal structures of hydrobenzamide and protonated amarine by HCl (meso-2,4,5-triphenyl-2-imidazoline hydrochloride ethanol solvate). This work revised the structures of the well known intermediates "hydrobenzamide" and "amarine" (Scheme 1). However, as shown in Scheme 1, the crystal structure of one of the important intermediates, "isoamarine (racemic-trans-2,4,5-triphenyl-2-imidazoline)" still remains unknown. In addition, there have been no reports of the chemistry of two intermediates, amarine and isoamarine, which serve a potential building block through N atom of imidazoline or its derivatives through 1,3-N atoms allylation. As a part of our studies of the olefin-copper(I) coordination polymers [5], we have determined the crystal structures of amarine (**1**) and isoamarine (**2**) and carried out the crystal structure determinations of the products of their 1,3-N atom allylation reactions and the copper(I) coordination chemistry of the allylation products with bromide anion. Herein, we report

---
[*] Corresponding author. Fax: +86 25 83317761/83314502.
E-mail address: xiongrg@netra.nju.edu.cn (R.-G. Xiong).
[1] These authors contributed equally to this work.

Scheme 1.

Scheme 2.
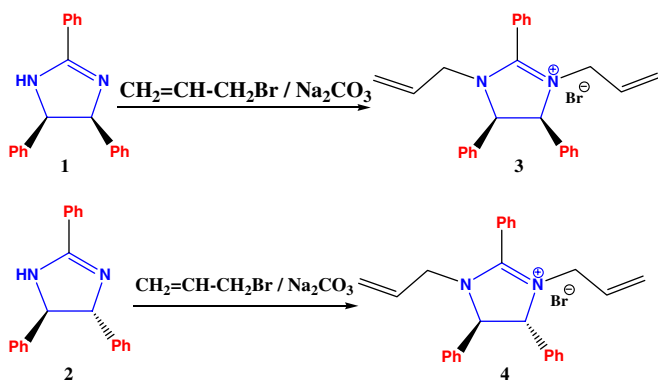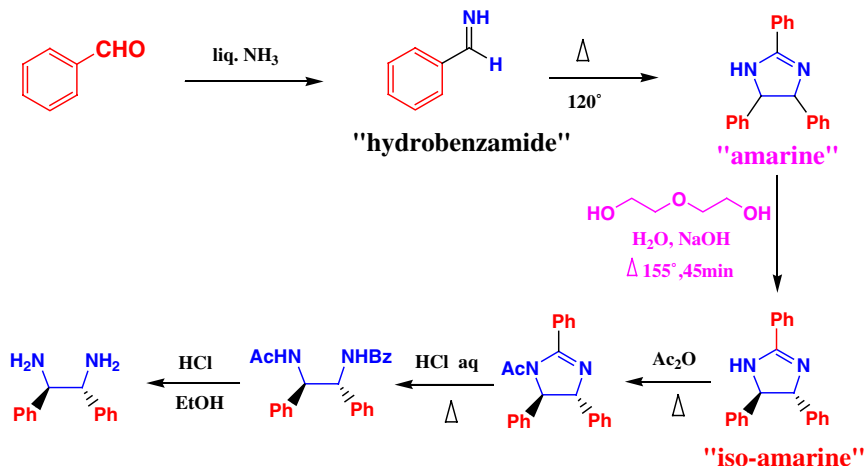
the synthesis and crystal structures of amarine (**1**) and isoamarine (**2**), and their 1,3-N atom allylation products as well as the fluorescent properties and crystal structures of the copper(I) complexes with their allylation bromide products as shown in Scheme 2.

2. Results and discussion

Amarine (**1**) and isoamarine (**2**) were prepared according to the literature reported by Corey et al. Their single crystals were obtained through the evaporation of solvent in air at room temperature. Crystal structure determination of **1** (Fig. 1(a)) shows that two amarine molecules and one water co-crystallize together through H-bonds and two phenyl rings are in *cis*-configuration, as the meso isomer. Compared to the crystal structure of the protonated **1**, the 1-N atom of imidazoline in **1** is un-protonated. As expected, the C–C and C–N bond distances (Table 1) in amarine are comparable to those found in protonated amarine [4].

The crystal structure of **2** (Fig. 2(a)), different from that found in **1**, reveals that two phenyl rings are *trans* and **2** is a racemic mixture. Similar to **1**, there is no protonated N atoms in **2**. The C–C and C–N bond lengths (Table 2)

are unexceptional and comparable to those in **1** and protonated **1** [4].

The reactions of **1** and **2** with allyl bromide afford 1,3-diallyl **1** [(**1**)(CH₂—CH=CH₂)₂]Br] (**3**) and 1,3-diallyl **2** [(**2**)(CH₂—CH=CH₂)₂]Br] (**4**), respectively, in the presence of Na₂CO₃ as shown in Scheme 2. Due to the difficulty of the formation of single crystals of **3** and **4**, we use PF₆⁻ anion to replace the Br⁻ anion in **3** and **4** successfully to determine their crystal structures of **3**-Br + PF₆ and **4**-Br + PF₆ as shown in Scheme 3.

Figs. 1(c) and 2(c) clearly confirms the above-mentioned diallylation reactions. Meanwhile, the *cis*- and *trans*-configurations of two phenyl rings in **3** and **4** still remain unchanged. As expected, the C–C and C–N bond lengths of **3**-Br + PF₆ and **4**-Br + PF₆ (Tables 3 and 4) are unexceptional and comparable to the corresponding **1** and **2**. Furthermore, the solvothermal reactions of **3** and **4** with CuBr give (**1**)₂(CH₂—CH=CH₂)₄(Cu₂Br₄) (**5**) and (**2**)(CH₂—CH=CH₂)₂(Cu₂Br₃) (**6**), respectively (Scheme 4). The crystal structure of **5** (Fig. 3) discloses that the olefin moiety of the allyl group does not take part in the coordination to Cu(I) probably due to the steric hindrance in which two phenyl groups and two olefin moieties in **3** are on the opposite plane of imidazole, and (**1**)(CH₂— CH= CH₂)₂ only acts as cation to balance the charge of dimeric Cu₂Br₄ anion in which the local coordination environment around Cu atom can be best described as three-coordinated planar trigonal. Interestingly, the crystal structure determination of **6** (Figs. 4 and 5) shows that the olefin moiety of the allyl group in (**2**)(CH₂—CH=CH₂)₂(Cu₂Br₃) participates in the coordination to Cu(I) to result in the formation of 1D infinite chain with two different local coordination geometry Cu atoms probably due to one of two phenyl rings being in the same plane of imidazole as one of two olefin moieties which is quite different from that found in **3** [6]. In one coordination geometry, Cu(I) is in a slightly distorted tetrahedron defined by two μ₂-bridging Br atoms, one terminal Br atom and the olefin moiety (Fig. 4). In the second coordination geometry, the
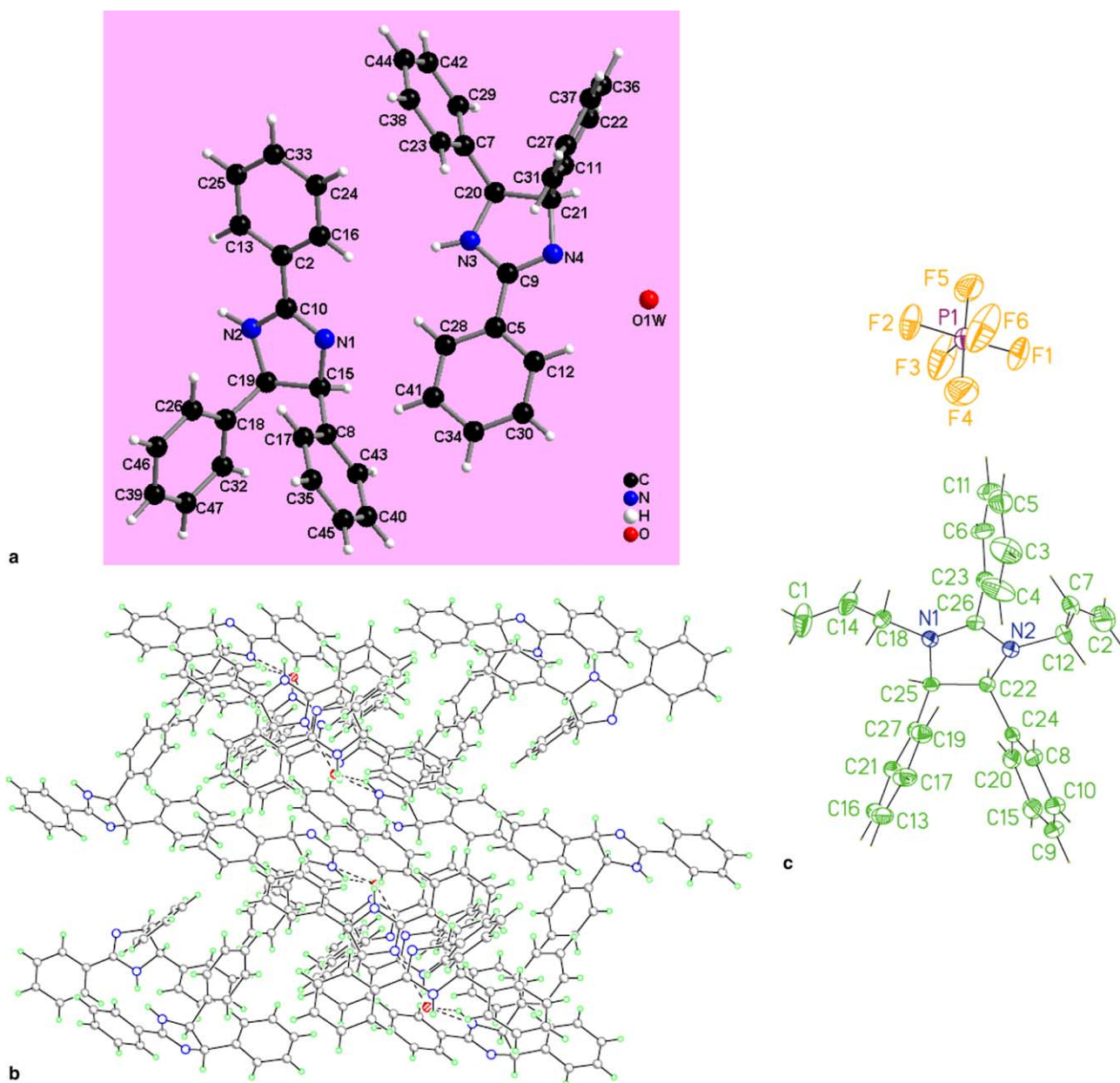
Fig. 1. (a) Perspective view of amarine (1) molecule. (b) Crystal packing view of 1 along a-axis. (c) Perspective view of 3-Br + PF₆ clearly showing two phenyl rings are cis-mode.

Table 1
Selected bond lengths (Å) and angles (°) for 1 (amarine)

N(1)–C(10)	1.326(4)	N(3)–C(20)	1.458(4)
N(1)–C(15)	1.472(3)	N(3)–C(9)	1.353(3)
N(2)–C(10)	1.312(4)	N(2)–C(19)	1.451(3)
C(9)–N(4)	1.279(4)	N(4)–C(21)	1.475(4)
C(15)–C(19)	1.567(4)	C(20)–C(21)	1.561(4)
C(10)–N(1)–C(15)	107.3(2)	C(10)–N(2)–C(19)	110.3(3)
N(1)–C(10)–N(2)	115.7(3)	N(1)–C(15)–C(19)	104.1(2)
C(8)–C(15)–C(19)	117.3(3)	C(18)–C(19)–C(15)	115.9(2)
N(2)–C(19)–C(15)	102.0(2)	C(7)–C(20)–C(21)	118.9(2)
N(4)–C(9)–N(3)	115.5(3)	C(9)–N(3)–C(20)	108.9(3)
C(9)–N(4)–C(21)	108.3(3)	C(11)–C(21)–C(20)	116.6(2)
N(3)–C(20)–C(21)	101.1(2)	N(4)–C(21)–C(20)	104.2(2)

coordination geometry around Cu(I) has a planar trigonal environment defined by one terminal Br atom, one μ₂-bridging Br atom and the olefin moiety (Fig. 4). Thus [(2)(CH₂─CH═CH₂)₂] cation acts as a bi-dentate spacer to link the two Cu(I) atoms. If [(2)(CH₂─CH═CH₂)₂] cation can be abbreviated as one straight line, a double infinite chain was formed in the 1D olefin copper(I) coordination polymer (6) as shown in Fig. 5(b) [6]. Furthermore, it can be found from crystal packing view of 6 that the terminal Br atom weakly coordinates to a Cu(I) atom (2.984 Å) to result in the formation of 2D network (Fig. 6(b)) [6]. As expected, two phenyl rings in 5 and 6 are in cis- and trans-configurations, respectively, from their crystal
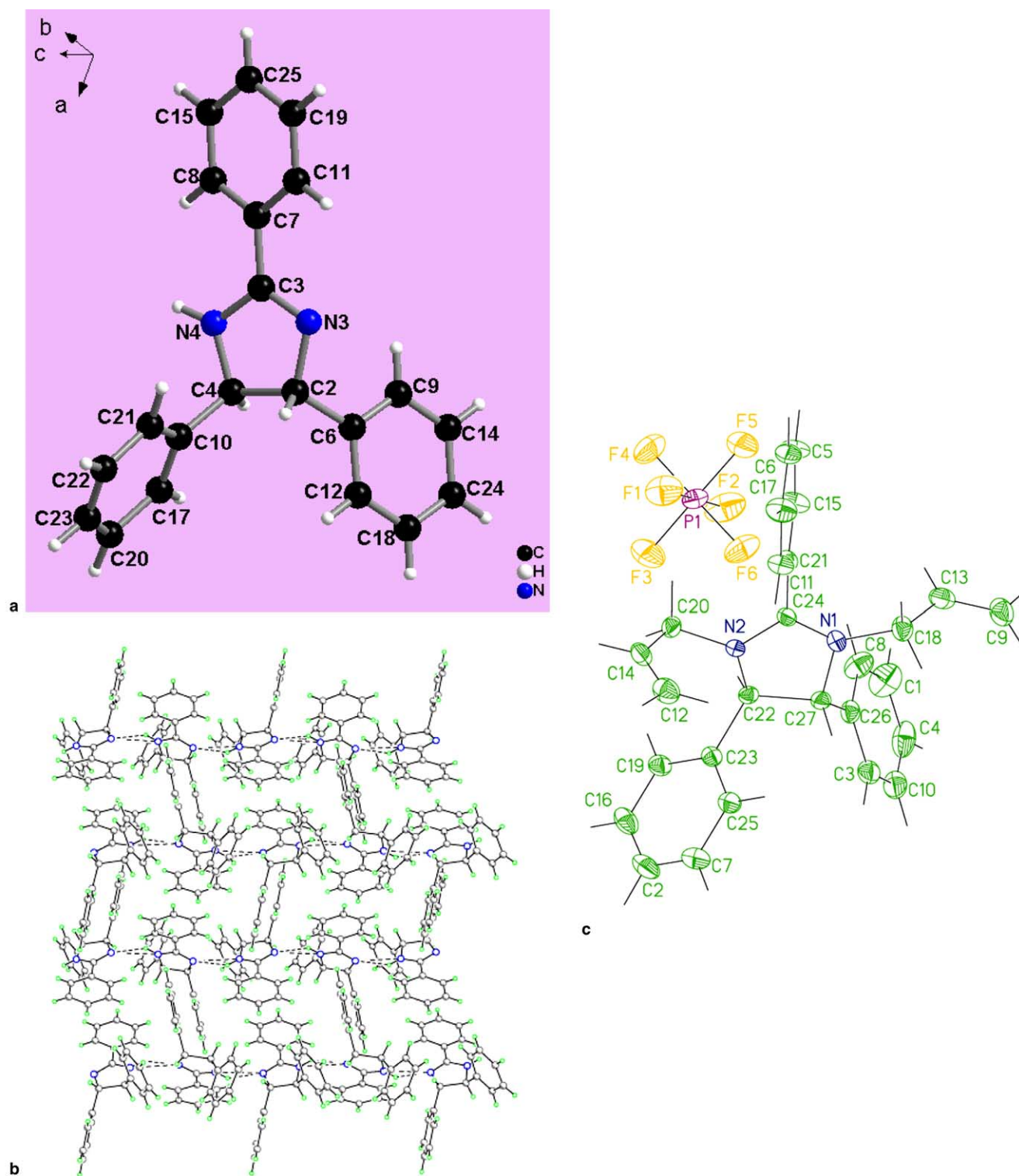
Fig. 2. (a) Perspective view of isoamarine (**2**). (b) Crystal packing view of **2** along *a*-axis. (c) Perspective view of **4**-Br + PF$_6$ clearly showing two phenyl rings are *trans*-mode.

structure determinations while the C–C and C–N bond distances are comparable to those in **1** and **2**, and unexceptional (Tables 5 and 6). The Cu–Br$_{terminal}$ bond distance (2.444 Å) is slightly longer than that of Cu–Br$_{\mu2-bridging}$ (2.001 Å) in **5**. Similarly, the Cu–Br$_{terminal}$ bond lengths

(2.3682 Å) are also slightly longer than the corresponding μ_2-bridging Cu–Br (2.4388–2.3905 Å) in **6**. The bond distances (1.325–1.336 Å) of the coordinated olefin moiety C=C in **6** are slightly longer than the corresponding bond lengths (1.284 Å) of the uncoordinated olefin moiety C=C

Table 2
Selected bond lengths (Å) and angles (°) for **2** (isoamarine)

N3 –C2	1.4679(19)	N3 –C3	1.2874(18)
N4 –C3	1.3569(19)	N4 –C4	1.438(2)
C2 –C4	1.565(2)		
C2 –N3 –C3	107.53(11)	C3 –N4 –C4	110.05(12)
N3 –C2 –C4	105.40(11)	C4 –C2 –C6	112.44(12)
N3 –C3 –N4	115.51(13)	N4 –C4 –C2	101.10(11)
C2 –C4 –C10	113.68(12)		
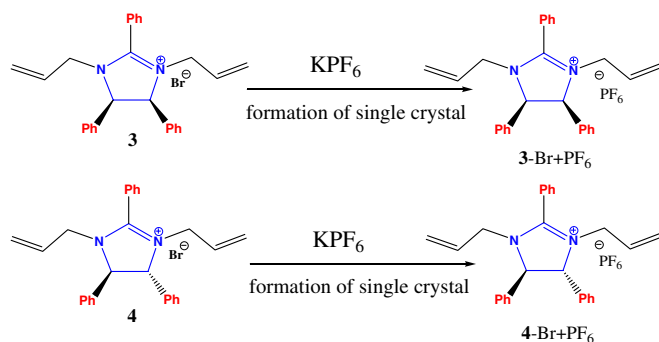
Scheme 3.

Table 3
Selected bond lengths (Å) and angles (°) for **3-Br + PF6**

P(1)–F(5)	1.464(5)	P(1)–F(3)	1.469(5)
P(1)–F(6)	1.471(5)	P(1)–F(4)	1.505(6)
P(1)–F(2)	1.553(4)	P(1)–F(1)	1.563(4)
N(2)–C(26)	1.330(5)	N(2)–C(12)	1.472(6)
N(2)–C(22)	1.470(5)	N(1)–C(26)	1.301(5)
N(1)–C(25)	1.465(5)		
F(5)–P(1)–F(3)	88.9(6)	F(5)–P(1)–F(6)	94.8(6)
F(3)–P(1)–F(6)	176.2(6)	F(5)–P(1)–F(4)	178.8(4)
F(3)–P(1)–F(4)	91.8(5)	F(6)–P(1)–F(4)	84.5(5)
F(5)–P(1)–F(2)	87.1(3)	F(3)–P(1)–F(2)	89.0(3)
F(6)–P(1)–F(2)	90.6(3)	F(4)–P(1)–F(2)	93.9(3)
F(5)–P(1)–F(1)	92.0(3)	F(3)–P(1)–F(1)	91.4(3)
F(6)–P(1)–F(1)	89.0(3)	F(4)–P(1)–F(1)	86.9(3)
F(2)–P(1)–F(1)	179.0(3)	C(26)–N(2)–C(12)	125.3(4)
C(26)–N(2)–C(22)	109.9(3)	C(12)–N(2)–C(22)	120.4(4)
C(26)–N(1)–C(25)	111.1(3)	C(26)–N(1)–C(18)	127.3(4)
C(25)–N(1)–C(18)	121.3(3)		

Table 4
Selected bond lengths (Å) and angles (°) for **4-Br + PF6**

P(1)–F(1)	1.556(4)	P(1)–F(3)	1.569(4)
P(1)–F(4)	1.567(4)	P(1)–F(6)	1.570(4)
P(1)–F(5)	1.568(4)	P(1)–F(2)	1.558(4)
N(1)–C(24)	1.312(5)	N(1)–C(27)	1.467(5)
N(1)–C(18)	1.491(6)	N(2)–C(24)	1.311(5)
N(2)–C(20)	1.457(6)	N(2)–C(22)	1.470(5)
F(1)–P(1)–F(3)	90.1(3)	F(1)–P(1)–F(4)	91.1(2)
F(3)–P(1)–F(4)	91.3(3)	F(1)–P(1)–F(6)	90.6(2)
F(3)–P(1)–F(6)	88.9(3)	F(4)–P(1)–F(6)	178.3(3)
F(1)–P(1)–F(5)	89.8(3)	F(3)–P(1)–F(5)	179.3(3)
F(4)–P(1)–F(5)	89.3(2)	F(6)–P(1)–F(5)	90.5(2)
F(1)–P(1)–F(2)	179.0(3)	F(3)–P(1)–F(2)	89.0(3)
F(4)–P(1)–F(2)	88.5(2)	F(6)–P(1)–F(2)	89.8(2)
F(5)–P(1)–F(2)	91.2(3)	C(24)–N(1)–C(27)	111.0(3)
C(24)–N(1)–C(18)	123.7(4)	C(27)–N(1)–C(18)	120.0(4)
C(24)–N(2)–C(20)	125.3(4)	C(24)–N(2)–C(22)	110.0(3)
C(20)–N(2)–C(22)	121.3(4)		
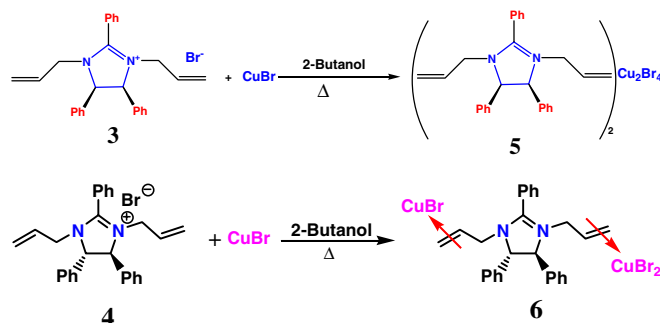
Scheme 4.

The luminescent spectra of **5** and **6** in the solid state at room temperature are shown in Fig. 7 with a maximum emission peak at ca. 570 nm (λ_{ex} = 363 nm) and 642 nm (λ_{ex} = 363 nm), respectively. The emission spectrum of the former (strong yellow-green fluorescent emission) is similar to those found in Cu_4I_4(pyridine)$_4$ (λ_{emax} = 580 nm) [8], [Cu(3,4'-bipyridine)(Br)]$_n$ (λ_{emax} = 580 nm) [9] and [Cu(3-PYA)]$_n$ as well as {[(2-PYA)Cu(I)]n(H$_2$O)}$_n$ (λ_{emax} = 580 nm, PYA = pyridylacrylate) [5]. Thus, the emission at 580 nm in **5** has been tentatively assigned to MLCT (metal-to-ligand charge transfer) since the fluorescent emission of the free ligand (**3**) is observed at about 470 nm. In addition, the shorter luminescent lifetime of **5** (ca. τ = 1.02 ns) in the solid state suggests its emission should be fluorescent emission. Interestingly, the emission spectrum of the later (**6**, strong red fluorescent emission) is similar to that found in {[bpy](4-hpya)Cu(I)}(BF$_4$)$_n$ (bpy = 2,2'-bipyridine, 4-hpya = *trans*-4-pyridylacrilic acid) with a maximum at ca. 647 nm (λ_{exc} = 250 nm). A clearly bathochromic shift occurs in **6** relative to [Cu$_4$I$_4$(py)] (λ_{emax} = 580 nm), [Cu(3,4-bpyBr)] (λ_{emax} = 580 nm) and **5** (λ_{emax} = 580 nm) which is probably due to π-back-donation from the filled metal d$_\pi$ orbital to the vacant antibonding π* orbital of the coordinated olefin
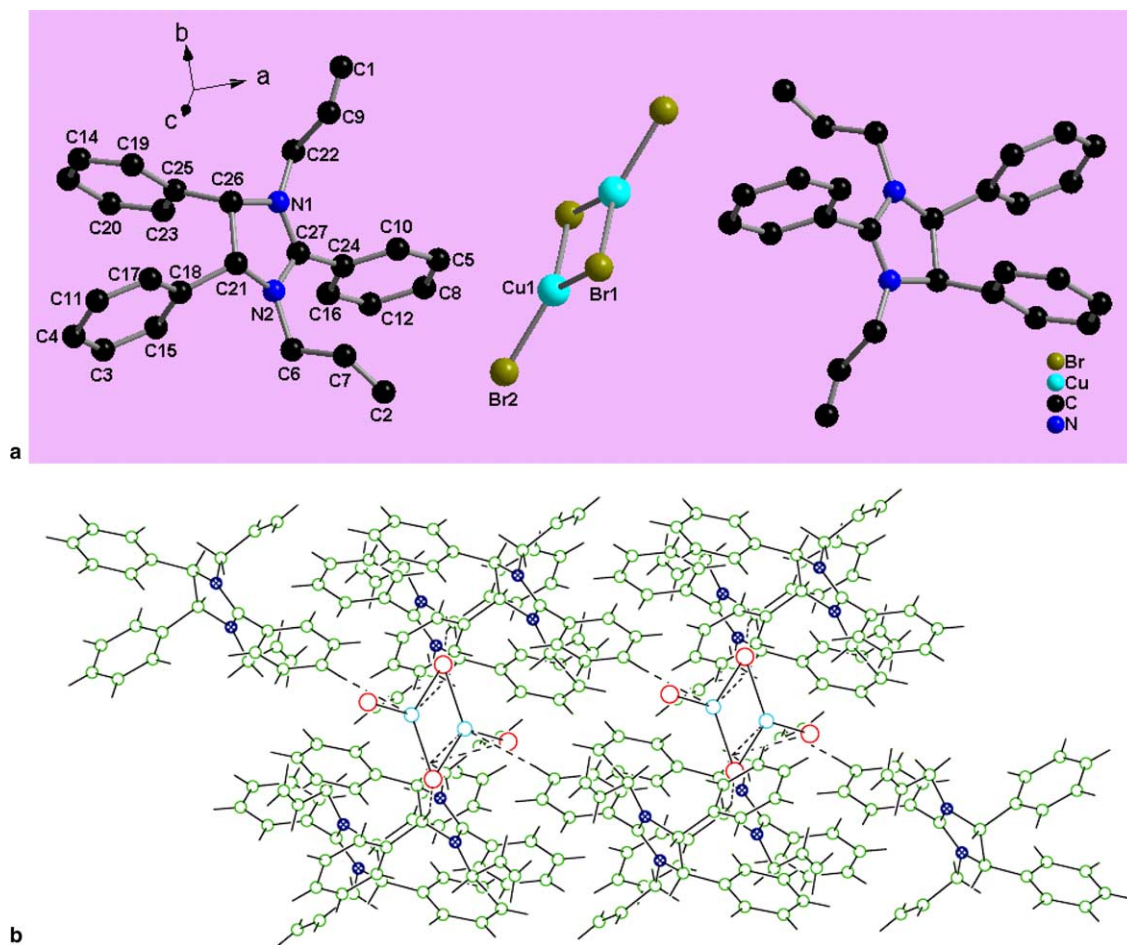
in **5**. Furthermore, the C–C bond distance for the coordinated olefin moiety **6** is slightly shorter than that found in [Cu$_2$Cl$_2$(C$_5$H$_8$)] (C$_5$H$_8$ = 2-methylbutadiene) (1.358(7) Å), [7c] [CuCl-(C$_5$H$_8$O)] (C$_5$H$_8$O = 1-penten-3-one) (1.383(8) Å) [7a] and [CuCl(C$_4$H$_6$O$_2$)] (C$_4$H$_6$O$_2$ = methylpropenoate) (1.370(8) Å) [6b] as well as {Cu(4-VPY)Cl}$_n$ (4-VPY = 4-vinylpyridine) (1.364(4) Å) [5d]. It is interesting to note that the C–C bond lengths of the coordinated olefin in the two copper(I) π-complexes Cu$_4$Cl$_4$L (1.33(2) Å) and Cu$_4$Br$_4$L (1.34(2) Å) (L = C$_7$H$_8$, 1,4-pentadiene) containing a Cu$_4$X$_4$ cubane core are almost comparable to those found in **6** [7e], and the Cu–C bond distances in Cu$_4$Cl$_4$L (2.10(1)–2.06(1) Å) and Cu$_4$Br$_4$L (2.05(1)–2.10(1) Å) are also similar to those found in **6** (2.082(8)–2.134(7) Å).

Fig. 3. (a) Perspective view of (**1**)$_2$(CH$_2$—CH=CH$_2$)$_4$(Cu$_2$Br$_4$) (**5**). (b) Crystal packing of **5** along *b*-axis.
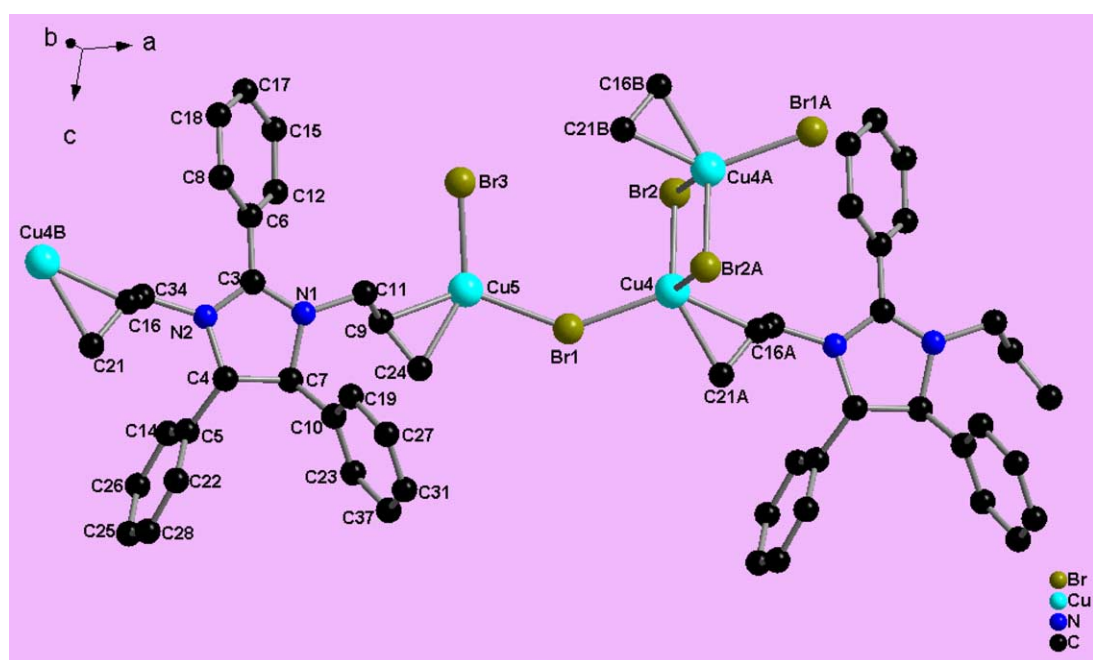
Fig. 4. Perspective of asymmetric unit of (**2**)(CH$_2$—CH=CH$_2$)$_2$(Cu$_2$Br$_3$) (**6**).
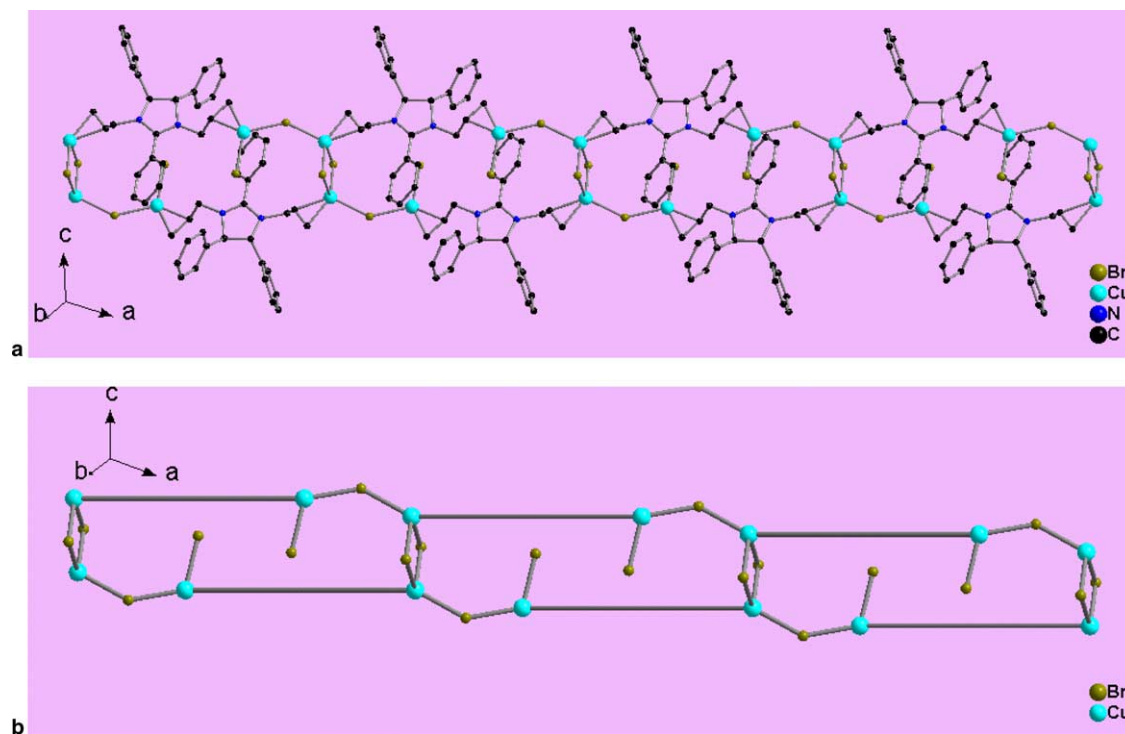
Fig. 5. (a) 1D chain representation of (**2**)(CH$_2$—CH=CH$_2$)$_2$(Cu$_2$Br$_3$) (**6**). (b) Simplified 1D chain representation of (**2**)(CH$_2$—CH=CH$_2$)$_2$(Cu$_2$Br$_3$) in which cation is abbreviated as a straight line.

[5a]. In addition, because the short lifetime (ca. $\tau = 1.50$ ns) and free ligand maximum emission peak being ca. 480 nm, the emission of **6** at 642 nm could be assigned to MLCT. Thus, the significant difference of fluorescent emission peak between Cu(I) complex without olefin moiety coordination and Cu(I) olefin coordination polymer has been observed and probably can be used for fluorescent sensing to discriminate two types of Cu(I) complexes.

In conclusion, we have successfully determined the crystal structures of amarine and isoamarine, intermediates in the preparation of 1,2-diphenyl-diaminoethane as well as their 1,-3-diallyation products. The coordination chemistry of Cu(I) with 1,3-diallylation amarine and isoamarine as ligands makes them useful in supramolecular chemistry as building blocks and solid state fluorescent sensing.

3. Experimental

3.1. The preparation of amarine (1) and isoamarine (2)

Compounds **1** and **2** were prepared from benzaldehye via hydrobenzamide according to the methods in the literatures reported by Corey et al. IR (cm^{-1}) for **1**: 3269(s), 3058(m), 3027(m), 2926(m), 1616(s), 1567(m), 1506(m), 1453(s), 1363(w), 1327(m) 1281(m), 1256(m), 1182(w), 1118(w), 1074(w), 1028(m), 1000(w), 922(m), 864(w), 744(s), 698(s), 576(m), 511(w); IR (cm^{-1}) for **2**: 3148(s), 3060(m), 3027(s), 2886(m), 1597(s), 1565(s), 1509(s), 1471(s), 1362(w), 1337(m), 1273(m), 1192(m), 1125(w), 1073(w),1022(m), 986(w), 922(w), 847(w), 757(s), 696(s), 643(m), 606(m), 536(m), 511(w).

3.2. Preparation of 3

A mixture of **1** (1.49 g, 5 mmol), allyl bromide (1.21 g, 10 mmol) and Na$_2$CO$_3$ (0.265 g, 2.5 mmol) in anhydrous CH$_2$Cl$_2$ (20 mL) were refluxed for 24 h. After cooling, the solution was filtered. The filtrate was concentrated under reduced pressure to give **3** with a yield of ca. 45% based on amarine. IR data (cm^{-1}): 3462(s), 3403(s), 3029(m), 2923(m), 2357(w), 1591(m), 1562(s), 1492(m), 1455(m), 1416(m), 1361(w), 1339(w), 1317(m), 1281(w), 1254(m), 1158(w), 1081(w), 1027(w), 993(m), 934(m), 790(m), 753(w), 700(s), 552(w), 514(w). $m/z = 379.4$. ^{1}H NMR (500 MHz, CDCl$_3$) δ 2.67 (N$^+$CH$_2$), δ 3.38 (NCH$_2$), δ 3.67 (N$^+$CH^{a}Ph), δ 4.51 (NCH^{b}Ph), δ 4.70 (=CH$_2$), δ 5.68 (N$^+$CH$_2$$CH$=CH$_2$), δ 6.04 (NCH$_2$$CH$=CH$_2$), δ 6.74–7.35 (15H, 3 × Ph). ^{13}C NMR (500 MHz, CDCl$_3$) δ 49.7 (N$^+$CH$_2$), δ 50.1 (NCH$_2$), δ 68.7 (N$^+$CH^{a}Ph), δ 78.3 (NCH^{b}Ph), δ 121.2 (NCH$_2$CH=CH_2), δ 122.4 (N$^+$CH$_2$CH=CH_2), δ 128.7–130.4 (18C,3 × Ph), δ 131.6 (NCH$_2$$CH$=CH$_2$), δ 133.3 (N$^+CH_2$$CH$=CH$_2$), δ 167 (PhC=N).

3.3. Preparation of 4

The procedure was identical to that used for **3** with a yield of ca. 35% based on isoamarine. IR data (cm^{-1}): 3423(s), 3031(m), 2924(m), 2357(w), 1732(w), 1561(s), 1489(w), 1447(m), 1421(m), 1338(m), 1277(m), 1224(w), 1076(w), 994(m), 929(m), 832(w), 757(m), 702(s), 550(w). $m/z = 379.4$. ^{1}H NMR (500 MHz, CDCl$_3$) δ 2.39 (N$^+$CH$_2$), δ 3.43 (NCH$_2$), δ 3.59 (N$^+$CH^{a}Ph), δ 4.40
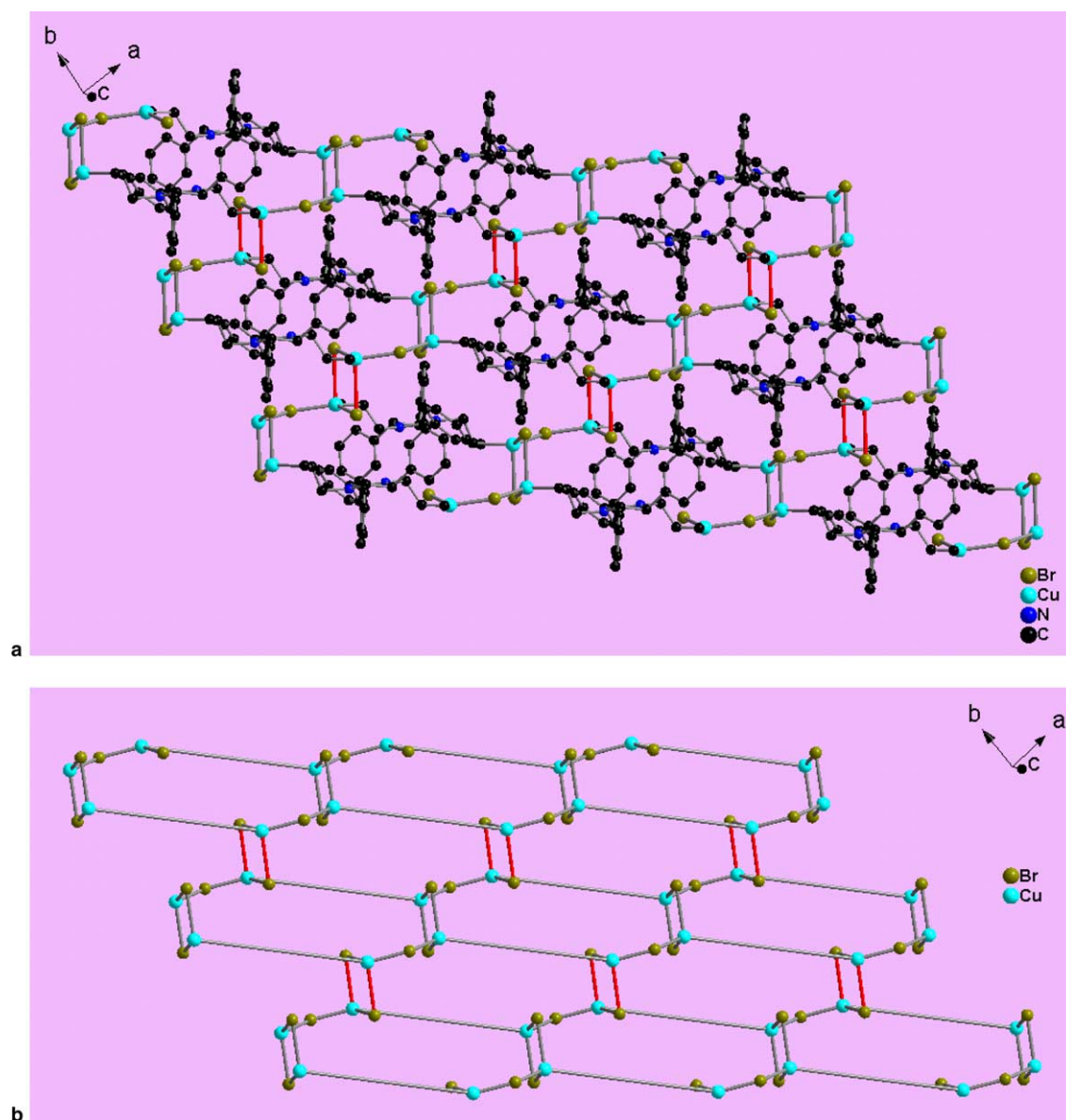
Fig. 6. (a) 2D network representation of $(\mathbf{2})(CH_2\!-\!CH\!=\!CH_2)_2(Cu_2Br_3)$ (**6**) through weak Cu–Br interaction (red line). (b) Simplified 2D representation of $(\mathbf{2})(CH_2\!-\!CH\!=\!CH_2)_2(Cu_2Br_3)$ (**6**) in which each 1D chain is connected by weak Cu–Br interaction and $(\mathbf{2})(CH_2\!-\!CH\!=\!CH_2)_2(Cu_2Br_3)$ is abbreviated as a straight line. (For interpretation of the reference to colour in this figure, the reader is referred to the web version of this article.)

Table 5
Selected bond lengths (Å) and angles (°) for **5**

Br(1)–Cu(1)	2.4222(9)	Br(2)–Cu(1)	2.2968(8)
C(27)–N(1)	1.311(5)	N(1)–C(26)	1.478(5)
C(27)–N(2)	1.321(5)	N(2)–C(21)	1.478(5)
C(26)–C(21)	1.576(6)	Cu(1)–Cu(1)#1	2.7842(13)
C(9)–C(1)	1.117(12)	C(7)–C(2)	1.284(2)
Cu(1)–Br(1)–Cu(1)#1	69.75(3)	Br(2)–Cu(1)–Br(1)	125.56(3)
Br(2)–Cu(1)–Br(1)#1	124.19(4)	Br(1)–Cu(1)–Br(1)#1	110.25(3)
N(1)–C(27)–N(2)	112.9(4)	C(27)–N(1)–C(26)	111.3(3)
N(1)–C(26)–C(21)	101.1(3)	C(27)–N(2)–C(21)	110.4(4)
N(2)–C(21)–C(26)	101.7(3)	C(18)–C(21)–C(26)	114.2(3)
C(25)–C(26)–C(21)	114.0(4)	C(6)–N(2)–C(21)	121.6(4)
C(22)–N(1)–C(26)	120.8(4)		

Symmetry transformations used to generate equivalent atoms: #1 $-x+1, -y, -z+1$.

(NCH^{b}Ph), δ 4.60 (=CH$_2$), δ 5.20 (CH=), δ 6.99–7.27 (15H,3 × Ph). ^{13}C NMR (500 MHz, CDCl$_3$) δ 49.7 (N$^+$CH$_2$), δ 50.1 (NCH$_2$), δ 73.2 (N$^+$CH^{a}Ph), δ 78.3 (NCH^{b}Ph), δ 121.1 (NCH$_2$CH=*CH$_2$*), δ 122.2 (N$^+$CH$_2$-CH=*CH$_2$*), δ 129.3–130.0 (18C,3 × Ph), δ 133.2 (NCH$_2$-*CH*=CH$_2$), δ 134.0 (N$^+$CH$_2$*CH*=CH$_2$), δ 167 (PhC=N).

3.4. Synthesis of 3-Br + PF$_6$

The mixture of **3** and KPF$_6$ in the solution of ethanol evaporates at the room temperature for three days to afford block-colorless single crystals. IR data (cm^{-1}): 3444(w), 3073(w), 1646(w), 1570(s), 1495(m), 1487(m), 1455(m), 1420(m), 1345(m), 1316(m), 1252(m), 1184(w), 1164(w),

Table 6
Selected bond lengths (Å) and angles (°) for **6**

Br(1)–Cu(5)	2.4204(13)	Br(1)–Cu(4)	2.4388(14)
Br(2)–Cu(4)#1	2.3905(15)	C(16)–Cu(4)#3	2.134(7)
Br(3)–Cu(5)	2.3682(15)	Cu(4)–C(21)#2	2.131(7)
Cu(5)–C(24)	2.082(8)	Cu(5)–C(9)	2.114(8)
N(1)–C(3)	1.317(9)	N(1)–C(7)	1.479(10)
N(2)–C(3)	1.323(10)	N(2)–C(4)	1.478(10)
C(4)–C(7)	1.541(10)	C(16)–C(21)	1.325(12)
C(9)–C(24)	1.336(11)		
Cu(5)–Br(1)–Cu(4)	139.30(5)	Br(1)–Cu(4)–Br(2)	101.71(5)
Cu(4)#1–Br(2)–Cu(4)	75.64(5)	Br(3)–Cu(5)–Br(1)	113.73(6)
Br(2)#1–Cu(4)–Br(1)	111.85(5)	Br(2)#1–Cu(4)–Br(2)	104.36(5)
C(3)–N(1)–C(11)	128.0(7)	C(3)–N(1)–C(7)	110.4(6)
C(3)–N(2)–C(34)	128.0(7)	C(3)–N(2)–C(4)	110.3(6)
N(1)–C(3)–N(2)	111.7(7)	N(2)–C(4)–C(5)	116.0(6)
N(2)–C(4)–C(7)	101.3(6)	C(10)–C(7)–C(4)	112.3(6)
C(5)–C(4)–C(7)	112.2(6)		

Symmetry transformations used to generate equivalent atoms: #1 $-x+2,-y+1,-z$, #2 $x+1,y-1,z$, #3 $x-1,y+1,z$.

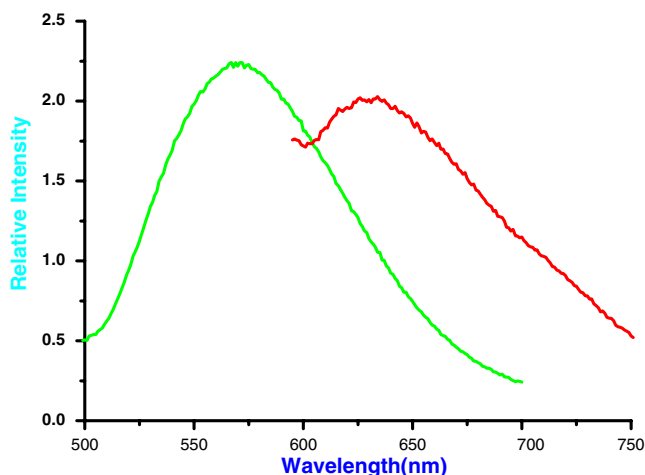Fig. 7. The fluorescent emission spectra of (**1**)$_2$(CH$_2$—CH═CH$_2$)$_4$(Cu$_2$Br$_4$) (**5**) and (**2**)(CH$_2$—CH═CH$_2$)$_2$(Cu$_2$Br$_3$) (**6**) at the solid state.

1121(w), 1098(w), 1081(w), 1027(w), 999(m), 934(s), 850(vs), 841(vs), 830(vs), 789(w), 698(m), 557(m).

3.5. Synthesis of **4**-Br + PF$_6$

The mixture of **4** and KPF$_6$ in the solution of ethanol evaporates at the room temperature for four days to afford block-colorless single crystals. IR data (cm^{-1}): 3421(w), 3035(w), 1647(w), 1565(s), 1486(w), 1454(m), 1417(m), 1355(m), 1336(m), 1277(m), 1230(w), 1203(w), 1133(w), 1076(w), 1031(w), 992(m), 839(vs), 755(s), 699(s), 639(w), 557(s).

3.6. Synthesis of **5**

Hydrothermal treatment of CuBr (2.0 mmol, 0.287 g) and **3** (1.0 mmol, 0.456 g) over four days at 60–70 °C yielded yellow block crystalline **5** (0.380 g, ca. 63.4% based on **3**).

Anal. Calc. for C$_{54}$H$_{54}$Br$_4$N$_4$Cu$_2$ (**5**): C, 53.79; H, 4.51; N, 4.65. Found: C, 53.54; H, 4.62; N, 4.57%. IR spectrum (KBr, cm^{-1}): (KBr, cm^{-1}): 3425(br, w), 3084(w), 3059(w), 3048(w), 2935(w), 2909(w), 1640(w), 1608(w), 16591(s), 1568(s), 1485(m), 1454(s), 1433(w), 1419(w), 1348(w), 1337(w), 1318(w), 1289(w), 1258(m), 1228(w), 1207(w), 1155(w), 1081(w), 1027 (w), 927(w), 1026(w), 993 (m), 926(m), 860(w), 789(s), 770(w), 754(w), 720(w), 698(s), 633(w), 614(w), 582(w), 547(w), 511 (w), 460(w), 424(w).

3.7. Synthesis of **6**

Hydrothermal treatment of CuBr (2.0 mmol, 0.287 g) and **4** (1.0 mmol, 0.456 g) over 4 days at 60–70 °C yielded yellow block crystalline **6** (0.332 g, ca. 55.4% based on **4**). Anal. Calc. for C$_{27}$H$_{27}$N$_2$Cu$_2$Br$_3$ (**6**): C, 43.35; H, 3.65; N, 3.75. Found: C, 43.18; H, 3.49; N 3.68%. IR spectrum (KBr, cm^{-1}): 3448(br, w), 3084(w), 3059(w), 3032(w), 3007(w), 2977(w), 2940(w), 2909(w), 1970(w), 1900(w), 1833(w), 1780(w), 1736(w), 1685(w), 1642(w), 1600(w), 1586(m), 1548(s), 1530(s), 1495(w), 1482(w), 1454(m), 1400(m), 1354(w), 1322(w), 1314(w), 1271(m), 1221(m), 1189(m), 1162(w), 1105(w), 1085(w), 1026(w), 1001(w), 971(w), 920 (m), 832(m), 780(m), 757(s), 701(s), 641(w), 615(w), 556(w), 516(w), 473(w), 449(w), 412(w).

3.8. Crystal data for **1**

C$_{42}$H$_{38}$N$_4$O, triclinic, space group, P$\bar{1}$, M_r = 614.76, a = 11.791(3), b = 12.232(3), c = 14.151(4) Å; α = 66.775(4), β = 81.245(5), γ = 64.868(5)°, V = 1697.8(7) Å^3, Z = 2, D_c = 1.203 Mg/m^3, μ = 0.073 mm^{-1}, S = 0.972, R_1 = 0.0623, wR_2 = 0.1689, T = 293 K, λ = 0.71073 Å.

3.9. Crystal data for **2**

C$_{21}$H$_{18}$N$_2$, monoclinic, space group, P2(1)/c, M_r = 298.37, a = 12.1743(18), b = 13.303(2), c = 10.1640 (16) Å; β = 92.876(4)°, V = 1644.1(4) Å^3, Z = 4, D_c = 1.205 Mg/m^3, μ = 0.071 mm^{-1}, S = 1.13, R_1 = 0.0746, wR_2 = 0.2291, T = 293 K, λ = 0.71073 Å.

3.10. Crystal data for **3**-Br + PF$_6$

C$_{27}$H$_{27}$F$_6$N$_2$P, monoclinic, space group, P2(1)/n, M_r = 524.48, a = 11.344(3), b = 15.858(4), c = 14.717(4) Å; α = 90, β = 90.494(5), γ = 90°, V = 2647.5(13) Å^3, Z = 4, D_c = 1.316 Mg/m^3, μ = 0.164 mm^{-1}, S = 1.289, R_1 = 0.0972, wR_2 = 0.2883, T = 293 K, λ = 0.71073 Å.

3.11. Crystal data for **4**-Br + PF$_6$

C$_{27}$H$_{27}$F$_6$N$_2$P, monoclinic, space group, Cc, M_r = 524.48, a = 14.856(2), b = 10.8075(16), c = 15.652(2) Å; α = 90, β = 93.123(3), γ = 90°, V = 2509.3(6) Å^3, Z = 4, D_c = 1.388 Mg/m^3, μ = 0.173 mm^{-1}, S = 0.810, R_1 = 0.0629, wR_2 = 0.1379, T = 293 K, λ = 0.71073 Å.

3.12. Crystal data for 5

$C_{54}H_{54}Br_4N_4Cu_2$, monoclinic, space group, $P2(1)/n$, $M_r = 1205.73$, $a = 10.3420(13)$, $b = 16.483(2)$, $c = 15.825(2)$ Å; $\alpha = 90$, $\beta = 106.998(3)$, $\gamma = 90°$, $V = 2579.7(6)$ Å^3, $Z = 2$, $D_c = 1.552$ Mg/m^3, $\mu = 3.961$ mm^{-1}, $S = 0.971$, $R_1 = 0.0487$, $wR_2 = 0.1401$, $T = 293$ K, $\lambda = 0.71073$ Å.

3.13. Crystal data for 6

$C_{27}H_{27}N_2Cu_2Br_3$, monoclinic, space group, $P2(1)/n$, $M_r = 746.32$, $a = 11.3900(12)$, $b = 9.5579(10)$, $c = 24.582(3)$ Å, $\alpha = 90$, $\beta = 101.621(3)$, $\gamma = 90°$, $V = 2621.3(5)$ Å^3, $Z = 4$, $D_c = 1.891$ Mg/m^3, $\mu = 6.215$ mm^{-1}, $S = 1.214$, $R_1 = 0.0793$, $wR_2 = 0.1912$, $T = 293$ K, $\lambda = 0.71073$ Å.

4. Supporting information available

Crystallographic CIF (excluding structure factors) and tables of atomic coordinates, thermal parameters, bond distances and angles for **1**, **2**, **3**-Br + PF$_6$, **4**-Br + PF$_6$, **5** and **6**.

References

[1] (a) K.D. Smet, A. Pleysier, I.F.J. Vankelecom, P.A. Jacobs, Chem. Eur. J. 9 (2003) 334;
(b) J. Krysiak, C. Lyon, A. Bacceiredo, H. Gornitzka, M. Mikolajczyk, G. Bertrand, Chem. Eur. J. 10 (2004) 1982.
[2] (a) F. Lake, C. Moberg, Tetrahedron Asymmetry 12 (2001) 755;
(b) M. Kojima, H. Taguchi, M. Tsuchimoto, K. Nakajima, Coord. Chem. Rev. 237 (2003) 183;
(c) S. Kezuka, T. Ikeno, T. Yamada, Org. Lett. 3 (2001) 1937.
[3] L. Cavallo, M.E. Cucciolito, A.D. Martino, F. Giordano, I. Orabona, A. Vitagaliano, Chem. Eur. J. 6 (2000) 1127.
[4] E.J. Corey, F.N.M. Kuhnle, Tetrahedron Lett. 38 (1997) 8631.
[5] (a) J. Zhang, R.-G. Xiong, J.-L. Zuo, X.-Z. You, Chem. Commun. (2000) 1495;
(b) J. Zhang, R.-G. Xiong, J.-L. Zuo, C.-M. Che, X.-Z. You, J. Chem. Soc., Dalton Trans. (2000) 2898;
(c) J. Zhang, R.-G. Xiong, X.-T. Chen, C.-M. Che, Z. Xue, X.-Z. You, Organometallics 20 (2001) 4118;

(d) J. Zhang, R.-G. Xiong, X.-T. Chen, Z. Xue, S.-M. Peng, X.-Z. You, Organometallics 21 (2002) 225;
(e) X. Xue, X.-S. Wang, R.-G. Xiong, B.F. Abrahams, X.-Z. You, C.-M. Che, Angew. Chem., Int. Ed. 41 (2002) 2944;
(f) Z.-R. Qu, Z.-F. Chen, J. Zhang, R.-G. Xiong, B.F. Abrahams, Z. Xue, Organometallics 22 (2003) 2814;
(g) Y.-R. Xie, X.-S. Wang, H. Zhao, J. Zhang, L.-H. Wang, C.-Y. Duan, R.-G. Xiong, X.-Z. You, Z.-L. Xue, Organometallics 22 (2003) 4396;
(h) Y.-H. Li, X.-S. Wang, H. Zhao, R.-X. Yuan, J. Zhang, R.-G. Xiong, X.-Z. You, H.-X. Ju, Z.-L. Xue, Inorg. Chem. 43 (2004) 712;
(i) Q. Ye, X.-S. Wang, H. Zhao, R.-G. Xiong, Chem. Soc. Rev. 34 (2005) 208.
[6] (a) M.J. Zaworotko, Chem. Soc. Rev. 23 (1994) 283;
(b) K.A. Hirsch, S.R. Wilson, J.S. Moore, Chem. Eur. J. 3 (1997) 765;
(c) C. Janiak, Angew. Chem., Int. Ed. 36 (1997) 1431;
(d) O.M. Yaghi, H. Li, C. Davis, D. Richardson, T.L. Groy, Acc. Chem. Res. 31 (1998) 474;
(e) S.R. Batten, R. Robson, Angew. Chem., Int. Ed. 37 (1998) 1460;
(f) A.J. Blake, N.R. Champness, P.A. Cooke, J.E.B. Nicolson, C. Wilson, J. Chem. Soc., Dalton Trans. (2000) 3811;
(g) L. Carlucci, G. Ciani, D.M. Proserpio, S. Rizzato, Chem. Eur. J. 8 (2002) 1520;
(h) O.R. Evans, W.-B. Lin, Acc. Chem. Res. 35 (2002) 511;
(i) D.-F. Sun, S.-Q. Ma, Y.-X. Ke, H.C. Zhou, Chem. Commun. (2005) 2663;
(j) S. Masaoka, G. Akiyama, S. Horike, S. Kitagawa, T. Ido, K. Endo, J. Am. Chem. Soc. 125 (2003) 1152;
(k) S. Masaoka, D. Tanaka, Y. Nankanishi, S. Kitagawa, Angew. Chem., Int. Ed. 43 (2004) 2530.
[7] (a) M. Hakansson, S. Jagner, J. Organomet. Chem. 336 (1987) 279;
(b) M. Hakansson, S. Jagner, J. Organomet. Chem. 361 (1989) 269;
(c) M. Hakansson, S. Jagner, Organometallics 10 (1991) 1317;
(d) M. Hakansson, S. Jagner, J. Organomet. Chem. 397 (1990) 383;
(e) M. Hakansson, S. Jagner, E. Clot, O. Eisenstein, Inorg. Chem. 31 (1992) 5389;
(f) M. Hakansson, K. Wettstrom, S. Jagner, J. Organomet. Chem. 421 (1991) 347.
[8] (a) V.W.-W. Yam, K.K.-W. Lo, Chem. Soc. Rev. 28 (1999) 323, and references therein;
(b) C.T. Cunningham, K.L.H. Cunningham, J.F. Michalec, D.R. McMillin, Inorg. Chem. 38 (1999) 4388;
(c) D.R. McMillin, K.M. McNett, Chem. Rev. 98 (1998) 1201;
(d) P.C. Ford, E. Cariati, J. Bourassa, Chem. Rev. 99 (1999) 3625, and references therein;
(e) P.D. Harvey, M. Drouin, T. Zhang, Inorg. Chem. 36 (1997) 4998;
(f) K.R. Kyle, C.K. Ryu, J.A. DiBenedetto, P.C. Ford, J. Am. Chem. Soc. 113 (1991) 2954;
(g) M. Henary, J.L. Wootton, S.I. Khan, J.I. Zink, Inorg. Chem. 36 (1997) 796;
(h) M.T. Miller, P.K. Gantzel, T.B. Karpishin, J. Am. Chem. Soc. 121 (1999) 4292.
[9] (a) H.-K. Fun, S.S.S. Raj, R.-G. Xiong, J.-L. Zuo, Z. Yu, X.-L. Zhu, X.-Z. You, J. Chem. Soc., Dalton Trans. (1999) 1711;
(b) X.-S. Wang, H. Zhao, Z.-R. Qu, Q. Ye, J. Zhang, R.-G. Xiong, X.-Z. You, H.-K. Fun, Inorg. Chem. 42 (2003) 5786.